

Sparse Traffic Grooming in Translucent Optical Networks

Gangxiang Shen, *Member, IEEE*, and Rodney S. Tucker, *Fellow, IEEE*

Abstract—Traffic grooming is important in the design and operation of translucent optical networks. This paper investigates sub-wavelength traffic grooming in a translucent optical network and shows how to take advantage of sub-wavelength traffic grooming capability of sparsely distributed opaque switch nodes. An efficient heuristic, called the virtual nodal degree ranked algorithm, is employed to select the best locations for opaque switch nodes. New mixed-integer linear programming (MILP) optimization models are developed to optimally groom sub-wavelength traffic demand in the translucent optical network. The models maximize served sub-wavelength traffic demand under a limited network capacity and minimize required wavelength capacity subject to the condition that all the traffic demands are served. The models are novel in optimization methodology because they incorporate both the *arc-node* and the *arc-path* multi-commodity optimization techniques for a single problem. Based on simulation studies, it is found that the performance of sub-wavelength traffic grooming of a translucent network is substantially improved by increasing the number of opaque switch nodes. For some network topologies, the performance saturates as the number of opaque switch nodes increases, though the phenomenon is not general for any type of network topology.

Index Terms—Amplified spontaneous emission (ASE) noise, opaque node placement, sparse traffic grooming, sub-wavelength traffic grooming, translucent optical network, transparent segment.

I. INTRODUCTION

TRAFFIC grooming is important to help reduce network design cost and improve network operational performance [1], [2]. In this paper, we consider sub-wavelength traffic grooming for a type of translucent optical network that is made up of a small set of opaque switch nodes and a set of transparent switch nodes [3]–[6]. Due to the embedded OEO conversion and electronic signal processing capabilities, an opaque switch node can provide various functions including signal regeneration, wavelength conversion and sub-wavelength traffic grooming. Most previous studies of translucent optical networks have concentrated on the advantages of signal regeneration and wavelength conversion of the opaque switch nodes [5]–[9]. However, the advantages of sub-wavelength traffic

grooming of opaque switches have not been fully explored in the literature.

This paper studies sub-wavelength traffic grooming in a translucent optical network. We show how sub-wavelength traffic grooming in sparsely-distributed opaque switch nodes in a translucent optical network can be used to groom the overall sub-wavelength traffic demand. This is a type of *sparse traffic grooming* [10]–[12]. Unlike most previous studies on traffic grooming, which are generally based on an *ideal* optical transport layer, the current study is more practical because it takes into account the limitation of physical-layer impairments [13].

We investigate two sub-problems, namely 1) *how to select the best locations for opaque switch nodes that provide the function of sub-wavelength traffic grooming* and 2) *how to optimally allocate wavelength capacity and groom sub-wavelength traffic demand subject to system constraints*. The system constraints considered here include wavelength capacity, sub-wavelength traffic demand, and physical-layer impairments. In the literature, many efforts have been dedicated to selecting the best locations for opaque switch nodes [5], [6] and optimally grooming sub-wavelength traffic demand [2]. By extending these existing efforts, we develop an approach for opaque switch node placement that incorporates physical-layer impairments and new mixed-integer linear programming (MILP) optimization models for sub-wavelength traffic grooming in translucent optical networks.

We examine how the number of opaque switch nodes and their placement affect the performance of traffic grooming. Our simulation studies indicate that with an increase in the number of opaque switch nodes, the performance of sub-wavelength traffic grooming is improved, as expected. Moreover, performance improvement saturates with an increasing number of opaque switch nodes under some networks topologies. However, this trend is not general for any type of topology. To the best of our knowledge, this work is the first in the field dedicated to sparse traffic grooming in a translucent optical network.

The rest of the paper is organized as follows. In Section II, we introduce the concepts of translucent optical network and sparse traffic grooming in a translucent optical network. In Section III, we present an algorithm to select the best locations for opaque switch node placement. In Section IV, we present MILP optimization models for sub-wavelength traffic grooming in a translucent optical network. The models maximize total served sub-wavelength traffic demand given a predefined network capacity and minimize required wavelength capacity given a predefined sub-wavelength traffic demand matrix. In

Manuscript received October 14, 2008; revised March 17, 2009. First published June 02, 2009; current version published August 28, 2009. This work was supported by the Australian Research Council (ARC).

G. Shen was with the University of Melbourne, Melbourne, Vic. 3010, Australia. He is now with Ciena Corporation, Linthicum, MD 21090 USA (e-mail: gshen@ciena.com, egxshen@gmail.com).

R. S. Tucker is with the Department Electrical and Electronic Engineering, University of Melbourne, VIC 3010, Australia (e-mail: r.tucker@ee.unimelb.edu.au).

Digital Object Identifier 10.1109/JLT.2009.2024174

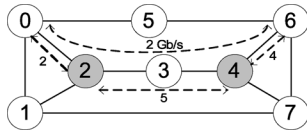


Fig. 1. Example of translucent optical network. Each lightpath carries 10-Gb/s capacity.

Section V, we evaluate the performance of sparse sub-wavelength traffic grooming of the translucent optical networks based on simulations.

II. TRAFFIC GROOMING IN TRANSLUCENT OPTICAL NETWORKS

Fig. 1 shows an example of a translucent optical network. The network consists of two opaque switch nodes, represented by grey circles, and a larger number of transparent switch nodes, represented by white circles. The opaque nodes provide signal regeneration, wavelength conversion, and sub-wavelength traffic grooming. In contrast, the transparent nodes simply switch lightpaths at the granularity of a wavelength. They do not disassemble or reassemble sub-wavelength traffic demand carried on bypassing lightpaths. However, they can add/drop sub-wavelength traffic demand locally at their add/drop ports on condition that appropriate sub-wavelength multiplexers and demultiplexers are present. A lightpath is a communication channel in the optical layer that carries a bandwidth equal to a full wavelength. Depending on the wavelength conversion capability in a network, a lightpath may be carried on the same wavelength throughout its route, or uses different wavelengths on different segments of its route if wavelength conversion capability is available on its intermediate nodes.

Depending on the number of consecutive lightpaths traversed by sub-wavelength traffic, there are two modes for sub-wavelength traffic grooming: *single hop grooming* and *multi-hop grooming* [2]. Single-hop grooming uses the capacity on a lightpath that is directly established between a pair of demand nodes to serve sub-wavelength traffic demand. In contrast, multi-hop grooming employs multiple consecutive lightpaths that connect a pair of nodes to serve sub-wavelength demand.

Fig. 1 includes examples of single-hop and multi-hop sub-wavelength traffic grooming. Assume 10-Gb/s lightpaths (0-2), (2-3-4), and (4-6) have been established (shown in Fig. 1 as dotted lines). Based on single-hop grooming, 2-, 5-, and 4-Gb/s sub-wavelength traffic demands are served respectively on the direct lightpaths between node pairs (0, 2), (2, 4), and (4, 6) with 8-, 5-, and 6-Gb/s free capacities remaining on the lightpaths, respectively. Due to the sub-wavelength traffic grooming capability at the opaque nodes 2 and 4, the free capacities on the three established lightpaths can be used to serve 2-Gb/s traffic demand between nodes 0 and 6 using multi-hop grooming.

Specifically, the traffic from node 0 to node 6 is first added at an optical add port of node 0 together with the traffic from node 0 to node 2. At node 2, the traffic destined for node 2 is dropped. Meanwhile, by taking advantage of the sub-wavelength traffic grooming capability of node 2, the traffic to node 6

is reassembled onto the lightpath between node 2 and node 4 with traffic from node 2 to node 4. At node 4, which is also capable of sub-wavelength traffic grooming, the same grooming process is performed to drop the traffic destined for node 4 and reassemble the traffic to node 6 onto the lightpath between nodes 4 and 6. The mixed traffic from node 0 and node 4 is eventually dropped at node 6 and separated, and the traffic between node 0 and node 6 is successfully served by using the free capacity on the existing lightpaths.

It is well known that multi-hop traffic grooming has the advantage of avoiding the establishment of direct lightpaths between node pairs when serving traffic demands, thereby saving optical add/drop ports and maximizing the capacity utilization of established lightpaths [2]. Fig. 1 provides an example to show this benefit. However, in a translucent network, how frequently multi-hop grooming can be applied is determined by the number of opaque nodes and their locations. For example, if there is only a single opaque node in Fig. 1 or there are no direct lightpaths established between nodes 4 and 6, then multi-hop traffic grooming between nodes 0 and 6 is impossible. Rather, a direct lightpath should be established between the two nodes. Thus, to exploit the benefits of multi-hop traffic grooming, it is important to find the best locations for the opaque nodes with sub-wavelength traffic grooming capability, and optimally allocate network wavelength capacity to establish lightpaths that can maximally serve sub-wavelength traffic demand.

For translucent optical networks, there are several key concepts and properties. First, the lightpath segment between any two neighboring opaque switch nodes is called a *transparent segment* [5]. In Fig. 1, the segment between node 2 and node 4 is a transparent segment. On each transparent segment, the constraint of wavelength continuity must be assured because only the two end nodes of the segment can convert wavelengths. Also, in a translucent optical network, before a transparent segment is established, its physical-layer signal quality must be taken into account to assure that the quality is always above a predefined threshold level [8]. Finally, because only the opaque nodes can groom sub-wavelength traffic, we define all the opaque nodes in a network as *the grooming node set*, and all the other nodes as *the non-grooming node set*. In Fig. 1, the grooming node set includes nodes 2 and 4, and the non-grooming node set includes all the other nodes.

III. ASE-NOISE-LIMITED OPAQUE NODE PLACEMENTS

A. ASE-Noise-Limited Impairment

ASE noise is one of the most fundamental aspects that constrain the maximal transparent reach of an optical signal [14]. In this study, we consider ASE noise as the dominant effect when modeling the physical-layer impairments.¹ A *pre* and *post-amplifier* pair are deployed before and after each OXC, respectively. Also, if the fiber link between two neighboring OXC nodes is long enough, inline optical amplifiers are deployed to

¹Without considering other impairments, the current study may underestimate the overall effect of physical-layer impairments. The framework can however be extended to include other physical-layer impairments as required.

boost the optical signal. ASE noise is accumulated when a lightpath passes an EDFA. The accumulated ASE noise is given by [15]

$$P_{\text{ase}}^o = P_{\text{ase}}^i G + 2n_{\text{sp}}(G - 1)hv_i B_o \quad (1)$$

where P_{ase}^i is the unpolarized power level of the accumulated ASE noise before a lightpath enters the EDFA, P_{ase}^o is the power level of the accumulated ASE noise after the lightpath traverses the EDFA, n_{sp} is the ASE noise factor, h is Plank's constant, v_i is the optical signal frequency, B_o is the receiver's optical bandwidth, and G is the gain of the optical amplifier.

At the receiver of a lightpath, we can estimate the Q -factor of the optical signal based on the accumulated ASE noise and received optical signal [15]. The Q -factor is widely used as a criterion to measure optical signal quality, which can decide whether a direct transparent lightpath can be established between a pair of nodes. Specifically, if the Q -factor is larger than a predefined threshold value (e.g., $Q > 7.0$), which guarantees a good bit error rate (BER), a direct transparent lightpath can be established; otherwise, signal regeneration is required in the middle of the lightpath.²

B. Opaque Node Placement

Strategies for opaque node placement are important to translucent network design and operation. A variety of algorithms have been proposed for locating the opaque switch nodes (or signal regenerators) in a translucent optical network [5]–[9]. In [7], the physical nodal degree of each optical switch node was selected as a weight to determine the priority of deploying 3R regenerators on these nodes. In [5], a criterion called the *transitional weight* was employed to determine the priority of deploying an opaque switch on each node. A transparent island division algorithm was proposed in [8] to deploy opaque switches on the boundaries of transparent islands. In [6], the OEO node placement problem was modeled as a Connected Dominating Sets (CDS) problem, in which OEO switches were placed at the nodes that are in the CDS. Similar to the concept of Connected Dominating Sets, in [9] an algorithm based on a criterion called the *virtual nodal degree* was developed. The algorithm selected the locations for opaque switch nodes based on the ability of a node to physically connect to other nodes within one lightpath hop.

In this paper, we extend the *virtual nodal degree* algorithm to select the opaque node locations. We called this algorithm the *virtual nodal degree ranked* algorithm. To determine whether a pair of nodes can be directly connected by a transparent lightpath, we take into account the ASE-noise impairment when computing Q -factor of a lightpath. Fig. 2 shows a flowchart of the extended *virtual nodal degree ranked* algorithm.

²In this study, we assume that the length of each fiber link is not so long as to require in-line 3R signal regeneration. However, if such a case occurs, the framework is general enough to cover this special case by taking the inline 3R signal regeneration into account when calculating Q -factor for a lightpath. However, it should be pointed out that inline 3R regeneration on a link does not bring any benefits to sub-wavelength traffic grooming since the inline regenerators are in the optical channel layer and there is no add/drop traffic at the locations of the regenerators.

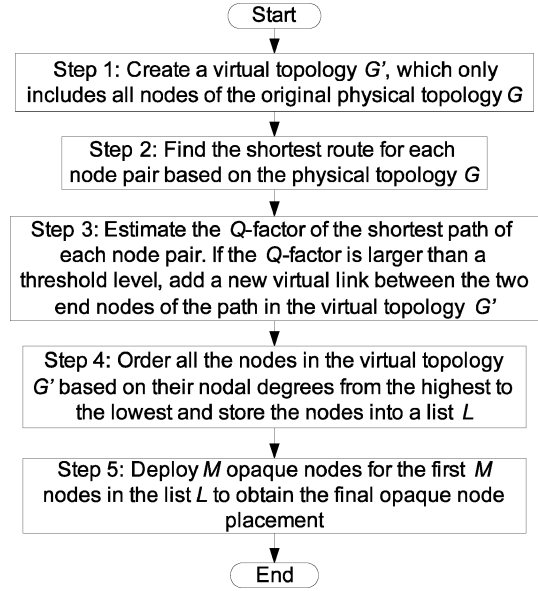


Fig. 2. Flowchart of opaque node placement in a translucent optical network based on the ranks of virtual nodal degrees.

Step 1 creates a virtual topology G' , which includes all nodes of the original topology G , but its link set is empty. Step 2 employs the shortest path routing algorithm to find the shortest route (in physical distance) between each node pair. Then for each of the routes, Step 3 employs the ASE-noise-limited physical-layer analysis model presented in Section III-A to decide whether the route is eligible to directly establish a transparent lightpath without requiring any intermediate 3R signal regeneration. The detailed rule for this is that if the estimated Q -factor of the lightpath is larger than a predefined threshold level (e.g., $Q > 7.0$), the direct transparent lightpath can be established between the node pair; otherwise, no such a lightpath is allowed.³ If a lightpath is established, a new virtual link is added to the virtual topology G' to connect the two end nodes of the lightpath. This process is repeated until all the shortest routes between the node pairs are examined. Finally, based on the virtual topology G' , Step 4 and Step 5 jointly select nodes from the highest nodal degree to the lowest nodal degree to deploy opaque switches until a predefined number M of opaque switches are placed. Here the number M is generally specified by the user and can be subject to the planning budget of the network.

IV. OPTIMIZATION MODELS FOR MAXIMAL SERVED TRAFFIC DEMAND AND MINIMUM REQUIRED WAVELENGTH CAPACITY

A. Discussion

The whole problem of sub-wavelength traffic grooming in a translucent optical network can be generally divided into two steps [2]: 1) *establishing virtual wavelength capacity pipes (also called virtual lightpath topology) between optical switch nodes* and 2) *aggregating sub-wavelength traffic demand into these*

³If there are any in-line 3R regenerations on the links traversed by the lightpath, the rule to determine whether the lightpath can be established is to see if any transparent segment (e.g., a segment between two neighboring inline 3R regenerators) on the route can pass a predefined Q -factor threshold level.

capacity pipes. The first step handles the issues of lightpath routing and wavelength assignment, which finds a virtual lightpath topology in the optical layer to serve sub-wavelength traffic demand. The second step routes sub-wavelength traffic demand on the established virtual lightpath topology.

We have the following key points in the network model. First, except at sparsely distributed opaque nodes which are assumed to have sub-wavelength traffic grooming capability, all the other nodes are transparent and can only add/drop their local sub-wavelength traffic, but cannot disassemble or reassemble sub-wavelength traffic on bypassing lightpaths. Second, only the opaque nodes can provide signal regeneration and wavelength conversion. All the other switch nodes can only transparently switch lightpaths at the granularity of a wavelength. Third, without losing generality, this study assumes that the traffic demands between node pairs are bidirectional. This assumption is usually justifiable for backbone transport networks.

For different network layers, we employ two types of multicommodity optimization techniques, i.e., the *arc-node* and *arc-path* multi-commodity optimization approaches, for a single network optimization problem. This approach is novel. We employ the arc-path technique to establish lightpaths over the fiber links and consequentially form a lightpath virtual topology, and the arc-node technique to route sub-wavelength traffic demand over the lightpath virtual topology. The arc-path technique for the lightpath establishment step provides the benefit of disintegrating the sub-step of determining qualified transparent segments (i.e., evaluating Q -values) from the capacity optimization, thereby significantly simplifying the model and improving computation efficiency.

B. MILP Optimization Models

In this section, we introduce mixed-integer linear programming (MILP) models that optimally aggregate sub-wavelength data traffic into high-capacity wavelength pipes. We optimize the traffic grooming problems from two perspectives. First, if network capacity (i.e., high-rate capacity pipes) is predefined, we maximize served low-rate sub-wavelength traffic demand over the capacity. Alternatively, we minimize the required wavelength channels on the condition that all the sub-wavelength traffic demands are served. We call the first *the maximal traffic serving model*, and the second *the minimum capacity model*. Both of these models have practical elegance. The maximal traffic serving model provides a way to maximize the utilization of the current deployed network capacity and thus postpone upgrading network capacity when network traffic increases. The minimum capacity model provides a straightforward way to minimize the network design cost, which is key to network design and planning.

In the paragraphs that follow, we define the sets, parameters, and variables used in the models. In particular, we use notations i and j to index the nodes in the optical layer and notations s and d to index the nodes in the sub-wavelength layer.

1) Sets:

- N Set of network nodes.
- N^{sd} Set of nodes that are able to aggregate or groom sub-wavelength traffic between s and d , which include source and destination node pair (s, d) by default and all the opaque nodes.
- S Set of network links.
- D Set of node pairs that have *lightpath* requests (i.e., end-to-end wavelength channels). These requests are essentially from the sub-wavelength layer that needs such lightpaths to be established to carry sub-wavelength traffic demands.
- P^r Set of eligible paths (or routes) for the lightpath demand request between node pair $r \in D$. Note that a path is eligible to establish a lightpath only if each transparent segment on the path can meet the Q -factor requirement (i.e., Q -factor > 7.0).
- $S^{r,p}$ Set of transparent segments on path p between node pair r . For example, in Fig. 1 if a lightpath is established from node 0 to node 6 via route 0-2-3-4-6, then the set of transparent segments of the lightpath includes segments of (0 to 2), (2 to 4), and (4 to 6).
- W Set of available wavelengths on each fiber link. We assume that each link has the same number of wavelengths.

2) Parameters:

- λ^{sd} Amount of requested end-to-end sub-wavelength traffic demand between node pair (s, d) .
- B Capacity (in Gb/s) that each wavelength (lightpath) can carry. For example, if a lightpath can carry a 10-Gb/s (i.e., OC-192) data rate, then B is equal to 10.
- $\xi_i^{r,p,s}$ Binary parameter related to lightpaths. It takes the value of one if the s th transparent segment of path p between node pair r traverses link i ; otherwise, zero.
- Δ_i Total number of local optical add/drop ports available at node i .
- θ_{ij}^r Relationship indicator between lightpath demands and node pairs. It takes the value of one if a lightpath demand r has an end node pair (i, j) ; otherwise, zero. Given the assumption of bi-directional lightpath demands, it is clear that $\theta_{ji}^r = \theta_{ij}^r$.

3) Variables:

- T^{sd} Served sub-wavelength traffic demand between node pair (s, d) .
- T_{ij}^{sd} Served sub-wavelength traffic demand between node pair (s, d) that traverses a (lightpath) virtual link between node pair (i, j) . Here “virtual link” and “lightpath” are exchangeable.

- C_{ij} Number of end-to-end lightpath channels established between node pair (i, j) .
- d_r Number of end-to-end lightpath channels that are established between node pair r . Later we will see that C_{ij} and d_r are connected through θ_{ij}^r .
- $f^{r,p}$ Number of end-to-end lightpath channels that are served on path p of node pair r .
- $\zeta_w^{r,p,s}$ Binary variable related to lightpaths. It takes the value of one if the s th transparent segment of path p of node pair r uses wavelength w ; otherwise, zero. Because no wavelength conversion is allowed on non-regeneration nodes, an identical wavelength is required on any transparent segment, which is termed *wavelength continuity*.
- O_w^i Takes the value of one if wavelength w on link i is used; otherwise, zero.
- U_w Takes the value of one if wavelength w is used on any one of the links in the network; otherwise, zero.

4) *Model 1: Maximize Served Sub-Wavelength Traffic Demand:* Objective:

$$\text{Maximize} \quad 0.5 * \sum_{s,d \in N^2: s \neq d} T^{sd} \quad (2)$$

$$\sum_{j \in N^{sd}: j \neq i} T_{ij}^{sd} - \sum_{j \in N^{sd}: j \neq i} T_{ji}^{sd} = \begin{cases} T^{sd}, & i = s \\ -T^{sd}, & i = d \\ 0, & \text{otherwise} \end{cases} \quad (3)$$

$$\forall s, d \in N^2 : s \neq d; i \in N^{sd} \quad (3)$$

$$T^{sd} \leq \lambda^{sd} \forall s, d \in N^2 : s \neq d \quad (4)$$

$$\sum_{s,d \in N^2: s \neq d} T_{ij}^{sd} \leq C_{ij} \cdot B \forall i, j \in N^2 : i \neq j \quad (5)$$

$$\sum_{j \in N: j \neq i} C_{ij} \leq \Delta_i \quad \forall i \in N \quad (6)$$

$$\sum_{i \in N: i \neq j} C_{ij} \leq \Delta_j \quad \forall j \in N \quad (7)$$

$$0.5 * \sum_{i,j \in N^2} \theta_{ij}^r \cdot C_{ij} = d_r \quad r \in D \quad (8)$$

$$d_r = \sum_{p \in P^r} f^{r,p} \quad \forall r \in D \quad (9)$$

$$f^{r,p} = \sum_{w \in W} \zeta_w^{r,p,s} \quad \forall s \in S^{r,p}, p \in P^r, r \in D \quad (10)$$

$$\sum_{s \in S^{r,p}, p \in P^r, r \in D} \zeta_w^{r,p,s} \cdot \xi_i^{r,p,s} \leq 1 \quad \forall i \in S, w \in W. \quad (11)$$

The objective (2) is to maximize the total served sub-wavelength traffic demand from the client layer. Constraint (3) grooms the sub-wavelength traffic from the sub-wavelength layer based on the lightpath virtual topology. Here the node set N^{sd} consists of all the opaque switch nodes and the two end nodes s and d of sub-wavelength traffic demand, as

only these nodes are able to multiplex/demultiplex or groom sub-wavelength traffic demand between node pair (s, d) . For example, in Fig. 2 for the sub-wavelength traffic demand between nodes 0 and 6, the node set N^{sd} is $\{0, 2, 4, 6\}$. Because the traffic demands between node pairs are bidirectional, for each sub-wavelength demand the model performs routing and grooming twice with one for each direction in constraint (3). To avoid doubly counting served (bidirectional) sub-wavelength demand, there is a factor of 0.5 in objective function (2).

Constraint (4) ensures that served sub-wavelength traffic demand would never exceed the demand requested. Constraint (5) ensures that enough lightpaths (wavelength capacity pipes) are established between nodes i and j such that all the sub-wavelength traffic demand that traverses the virtual link (i, j) can be fully supported. Constraints (6) and (7) say that the maximal number of lightpaths starting or ending at a node is subject to the number of allowed lightpath add/drop ports at the node. Constraint (8) makes a mapping between two lightpath demand formats, which are used in the *arc-node* and *arc-path* multi-commodity models, respectively. In addition, because of bidirectional traffic assumption, both node pairs (i, j) and (j, i) under the *arc-node* model can be mapped to a common lightpath demand r under the *arc-path* model. Constraint (9) ensures that the lightpath demand between node pair r is served by path set P^r . Constraint (10) says that each path segment should carry the same number of lightpaths as that of the whole path. Constraint (11) ensures that any wavelength on a fiber link can only be used by a single lightpath segment.

5) *Model 2: Minimize Required Wavelength Capacity:* Objective:

$$\text{Minimize} \quad \sum_{w \in W} U_w + \alpha \sum_{i \in S, w \in W} O_w^i \quad (12)$$

$$\sum_{j \in N^{sd}: j \neq i} T_{ij}^{sd} - \sum_{j \in N^{sd}: j \neq i} T_{ji}^{sd} = \begin{cases} \lambda^{sd}, & i = s \\ -\lambda^{sd}, & i = d \\ 0, & \text{otherwise} \end{cases} \quad (13)$$

$$\forall s, d \in N^2 : s \neq d; i \in N^{sd}.$$

Constraints (5)-(10)

$$\sum_{s \in S^{r,p}, p \in P^r, r \in D} \zeta_w^{r,p,s} \cdot \xi_i^{r,p,s} = O_w^i \quad \forall i \in S, w \in W \quad (14)$$

$$U_w \geq O_w^i \quad \forall i \in S, w \in W. \quad (15)$$

The objective of this model is to minimize the maximal wavelength number on the fiber links as well as the total wavelength capacity in the whole network. α in (12) is a weight factor. By setting a small α (i.e., 10^{-5}), the maximal wavelength number on the fiber links becomes a primary objective to minimize. Constraint (13) ensures that all the sub-wavelength traffic demand from the client layer is served by the lightpath links on the lightpath virtual topology. Constraint (14) determines the utilization state of each wavelength on each fiber link. Constraint (15) finds whether wavelength w is used on any links in the network.

TABLE I
SYSTEM PARAMETERS USED IN THE SIMULATION STUDIES

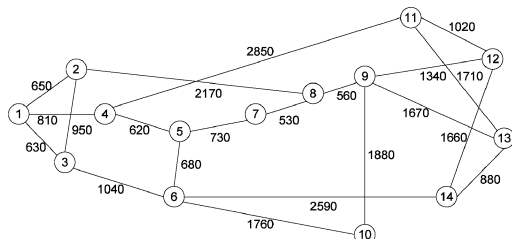
Parameter	Value
Channel data rate	10 Gb/s
Receiver's electronic bandwidth (B_e)	7 GHz
Receiver's optical bandwidth (B_o)	50 GHz
Receiver's responsivity (R)	0.95 Amp/W
Receiver's thermal noise current (I_{th})	3.8×10^{-12} Amp/ $\sqrt{\text{Hz}}$
OXC demux/mux insertion loss [16]	2 dB
OXC optical switch insertion loss [17]	5 dB
EDFA spontaneous factor (n_{sp})	1.41
Frequency of central wavelength (ν_c)	1.94×10^{14} Hz
Fiber loss factor (α)	0.25 dB/km
Maximal amplification span distance	80 km
Q -factor threshold	7.0
Amplified signal power after EDFA (P_{sg})	0 dBm

TABLE II
OPAQUE NODE LOCATIONS IN NSFNET

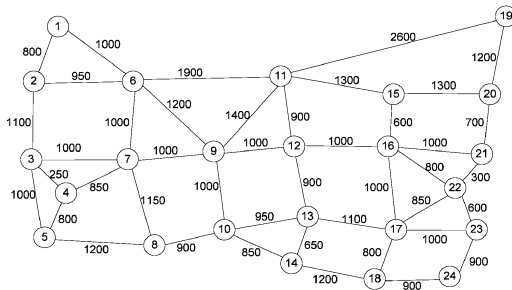
Number of opaque nodes	Locations of opaque nodes
3	7, 8, 9
5	5, 6, 7, 8, 9
7	1, 4, 5, 6, 7, 8, 9
9	1, 3, 4, 5, 6, 7, 8, 9, 10

TABLE III
OPAQUE NODE LOCATIONS IN US BACKBONE NETWORK

Number of opaque nodes	Locations of opaque nodes
4	9, 10, 11, 12
8	9, 10, 11, 12, 13, 14, 15, 16
12	7, 8, 9, 10, 11, 12, 13, 14, 15, 16, 17, 18



(a) 14-node 21-link NSFNET



(b) 24-node 43-link US backbone network

Fig. 3. Test networks. (a) 14-node 21-link NSFNET. (b) 24-node 43-link US backbone network.

V. SIMULATIONS AND PERFORMANCE EVALUATION

A. System Parameters and Test Networks

The physical-layer parameters used to estimate Q -factor for each lightpath and segment are shown in Table I. Specifically, each lightpath is assumed to be at 10 Gb/s. The maximal amplification span is set to be 80 km and the optical signal power on each channel is amplified to 0 dBm after each amplifier. The threshold Q -factor is set to be 7.0. Only if an end-to-end lightpath has a Q -factor greater than the threshold, can it be established between the node pair.

Our test networks include a 14-node 21-link NSFNET network and a 24-node 43-link US backbone network as shown in Fig. 3. The number shown by each link in the figure indicates the physical length of the link in km, which is a key parameter

when calculating Q -factors.⁴ Based on the opaque node placement algorithm shown in Fig. 2, we find the opaque node locations for different numbers of allowed opaque switch nodes, which are listed out in Tables II and III, respectively, for the two test networks. In particular, a transparent optical network can be considered as a special translucent optical network with zero opaque switch nodes, and an opaque network can be considered as a special translucent optical network with opaque switches on all the network nodes.

B. Performance Analyses

For performance evaluation, sub-wavelength traffic demand matrices are randomly generated. We assume that each node pair has a random end-to-end sub-wavelength traffic demand, whose amount is distributed within a range from 10 Gb/s to 40 Gb/s. For an entire network, there is a total end-to-end sub-wavelength traffic demand of 1820 Gb/s and 5520 Gb/s in the NSFNET network and the US backbone network, respectively.

To establish lightpaths, the K -shortest path routing algorithm (based on physical distance) is applied to find a set of candidate routes for each node pair. The following rule is applied to examine whether a route in the found K shortest ones is eligible to establish a lightpath. Specifically, the Q -factor is examined for each of the transparent segments on each of the routes to determine whether a route is eligible to establish a lightpath. If a predefined Q -factor threshold level cannot be met on any transparent segment, the examined route should be removed from the candidate route set. As a result, the remaining routes (after the removals) make up an eligible route set that can be used to establish lightpaths in the optimization model.

Optimization studies were performed under different network scenarios ranging from transparent, translucent with different numbers of opaque nodes, and opaque networks. We considered both the *minimum capacity model* and *maximal traffic serving model*. We minimize the required number of wavelengths to fully serve given sub-wavelength traffic demand, and maximize served sub-wavelength traffic demand if network capacity has been predefined. To establish lightpaths between node pairs, we

⁴In the simulation tests, we assume that there are no so long links in the test networks that require in-line 3R signal regeneration.

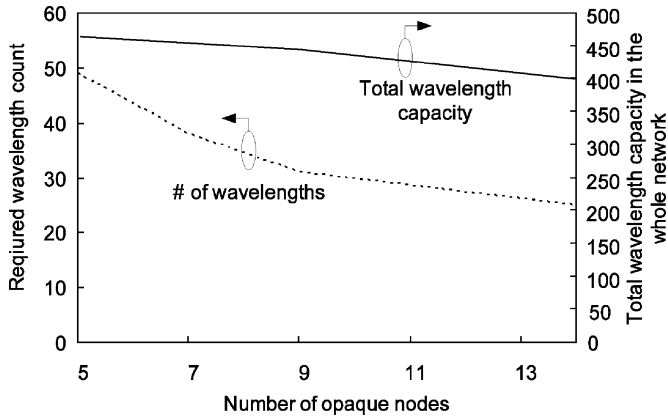


Fig. 4. Number of required wavelengths and total wavelength capacity in the network (NSFNET).

assume that there are maximal $K = 2$ candidate routes that can be used and participate in the Q -factor test. In addition, we ignored the constraint of maximal number of add/drop ports at each switch node in our simulations for fast MILP solutions. All the optimization cases were solved by a commercial software package AMPL/CPLEX of version 10 on a desktop with a 3.39-GHz CPU and 1 G of RAM.

1) *Minimum Wavelength Capacity*: Fig. 4⁵ shows the results of the minimum required wavelength capacity in the NSFNET network when all the sub-wavelength traffic demands are served. The curve associated with the left y -axis shows the required number of wavelengths to fully serve the traffic demands (i.e., $\sum_{w \in W} U_w$), and the curve associated with the right y -axis shows the total wavelength capacity in the whole network (i.e., $\sum_{i \in S, w \in W} O_w^i$). It can be seen in Fig. 4 that from a few opaque nodes (i.e., translucent networks) to 14 opaque nodes (i.e., an opaque network), both the required number of wavelengths and the total network capacity decrease. This is because the increase in the number of opaque nodes provides more flexibility and opportunities for sub-wavelength traffic grooming, signal regeneration, and wavelength conversion. In addition, comparing the two curves, it can be seen that the number of required wavelengths decreases more rapidly, while the total wavelength capacity does not decrease substantially. Specifically, moving from a translucent optical network with five opaque nodes to a fully opaque network, the number of required wavelengths decreases from 49 to 25. In contrast, there is only 16% reduction of total wavelength capacity in transitioning from the five-opaque-node translucent network to the opaque network.

2) *Maximal Served Traffic Demand*: Given that the deployed network capacity is limited, we are also interested in maximizing served end-to-end sub-wavelength traffic demand. For this sub-study, simulations were conducted for the NSFNET network. Assuming the same sub-wavelength traffic demand matrix as in the previous capacity-minimization study, we try to maximally satisfy sub-wavelength traffic requests. We assumed that each network link has 25 wavelengths, which are

⁵No solution (with all the simulated sub-wavelength demands served) can be found when there are only three opaque nodes as shown in Table II. Thus, the number of opaque nodes starts from five in the x -axis.

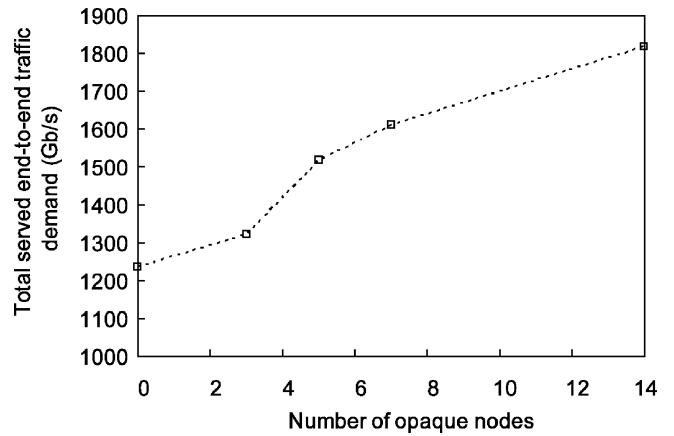


Fig. 5. Impact of network transluency on the total served end-to-end sub-wavelength traffic demand (NSFNET, 25 wavelengths per link).

the required minimum wavelengths to serve all the sub-wavelength traffic demands under an opaque network (see Fig. 4). Based on this capacity, simulation studies were performed to find the maximal served sub-wavelength traffic demand for various translucent network scenarios which have different opaque switch nodes.

Fig. 5 shows the simulation results for the NSFNET network. We can see that with the increase of the number of opaque nodes, the total served end-to-end sub-wavelength traffic demand (Gb/s) increases. As before, it can be explained by the fact that a larger number of opaque nodes provide more flexibility and opportunities for sub-wavelength traffic grooming, signal regeneration, and wavelength conversion.

Similar simulation studies were performed for the larger US backbone network and the results are shown in Fig. 6.⁶ The same observation can be found that the increase of opaque nodes in the network helps improve the network performance, i.e., more sub-wavelength traffic demand is served. Interestingly, we also observe a saturation phenomenon between the number of opaque nodes and the maximal served end-to-end sub-wavelength traffic demand. From a transparent network without any intermediate traffic grooming capability to a small increase of the number of opaque nodes (e.g., to 4 opaque nodes), we find a significant performance improvement, about 24% more traffic demand served. Nonetheless, after 4 opaque nodes, any further increase of opaque nodes in the network seems to only bring minimal performance improvement. Such a saturation phenomenon is however not found in the NSFNET network. Some explanations for this difference are as follows.

The US backbone network has a *planar* topology without any shortcut links. The nodes in the middle of the network such as nodes (9, 10, and 11) are clearly the strongest contenders to function as signal regeneration nodes (i.e., opaque nodes) for the lightpaths between the nodes on the west and east sides. In contrast, the NSFNET network is a different type of topology, which has several long short-cut links, e.g., links (4-11) and (2-8). These shortcut links blur the clear distinction of which

⁶Due to the limited wavelength capacity, i.e., 40 wavelengths per fiber, the total served demand in the US network does not reach 5520 Gb/s. If more wavelengths are carried on each fiber link, all the sub-wavelength traffic demands can be fully served.

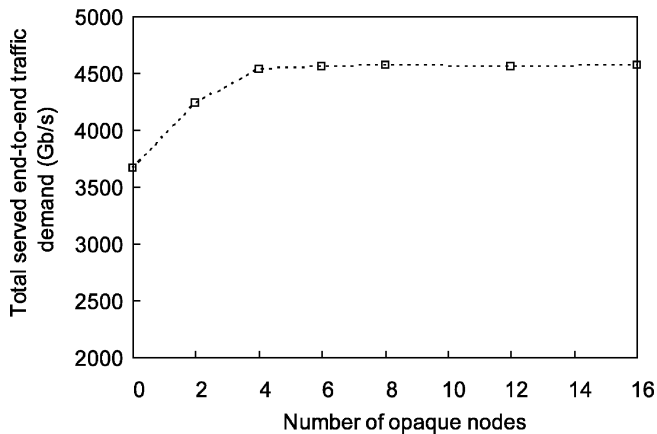


Fig. 6. Impact of network transluency on the total served end-to-end traffic demand (US backbone, 40 wavelengths per link).

nodes should have higher priorities to function as signal regeneration nodes. Thus, when the same percentage of opaque nodes is added to an initial transparent network, the performance improvement in the NSFNET network is not as dramatic as that in the US backbone network.

For future research, it would be useful to explore how the network topology can affect the performance of sub-wavelength traffic grooming in translucent networks. While a detailed consideration of this is beyond the scope of the present paper, we are in a position to make the following preliminary observations. We believe that the saturation phenomenon as shown can be expected for a network with a *planar* topology like the US backbone network, while if a network topology has many *short-cut* links such as links (4-11) and (2-8) in NSFNET, no clear saturation trends would be expected.

In addition, in the simulation studies we assumed that the sub-wavelength traffic demands are based on a uniformly random distribution. Traffic demands with different distribution patterns may lead to different grooming results. Thus, it is also interesting to explore how traffic demand distributions or patterns can affect the performance of sub-wavelength traffic grooming in translucent networks.

3) *Effect of Number of Candidate Routes*: All the results presented so far are based on the assumption that there are up to two candidate routes between each node pair for establishing lightpaths in the optical layer. The number of candidate routes examined for the eligibility of establishing lightpaths can be another important factor that affects the performance of sub-wavelength traffic grooming. We have evaluated the effect by changing the number of tested candidate routes between each node pair. It is anticipated that a larger number of candidate routes can generate more qualified end-to-end routes that satisfy a predefined Q -factor requirement, and provide more opportunities for establishing direct lightpaths to serve more sub-wavelength traffic demand.

Fig. 7 shows how the total served end-to-end sub-wavelength traffic demand changes with an increasing number of candidate routes for the NSFNET network. It can be seen that the increase in the number of candidate routes does benefit sub-wavelength traffic grooming. However, the performance improve-

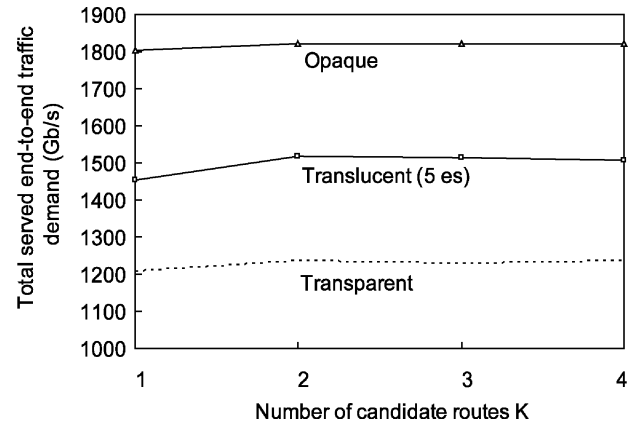


Fig. 7. Impact of the number of candidate routes K on the total served end-to-end sub-wavelength traffic demand (NSFNET, 25 wavelengths per link). The translucent network has five opaque nodes.

ment is minimal even if more candidate routes are considered when the number of candidate routes is more than two. This therefore implies that the performance of sub-wavelength traffic grooming in translucent networks saturates with an increasing number of candidate routes.

VI. CONCLUSION

We studied sub-wavelength traffic grooming in a translucent optical network. We have developed the virtual nodal degree ranked algorithm for opaque node placement and the novel MILP-based models for sub-wavelength traffic grooming for translucent optical networks. The models maximize served sub-wavelength traffic demand and minimize required wavelength capacity. Our simulation studies show that the performance of sub-wavelength traffic grooming is improved with an increasing number of opaque switch nodes. Also, for some network topologies (with planar graphs) such as the US backbone network, the performance improvement saturates as the number of opaque switch nodes increases. Further research is needed to evaluate how network topologies can affect the performance of sub-wavelength traffic grooming in a translucent optical network.

REFERENCES

- [1] O. Gerstel, R. Ramaswami, and G. H. Sasaki, "Cost-effective traffic grooming in WDM rings," *IEEE/ACM Trans. Netw.*, vol. 8, pp. 618–630, Oct. 2000.
- [2] K. Zhu and B. Mukherjee, "Traffic grooming in an optical WDM mesh network," *IEEE J. Sel. Areas Commun.*, vol. 20, no. 1, pp. 122–133, Jan. 2002.
- [3] B. Ramamurthy *et al.*, "Transparent vs. opaque vs. translucent wavelength-routed optical networks," in *Proc. OFC'99*, vol. 1, pp. 59–61.
- [4] G. Shen and R. S. Tucker, "Translucent optical networks: The way forward," *IEEE Commun. Mag.*, vol. 45, no. 2, pp. 48–54, Feb. 2007.
- [5] G. Shen *et al.*, "Sparse placement of electronic switching nodes for low blocking in translucent optical networks," *J. Opt. Netw.*, vol. 1, no. 12, pp. 424–441, Dec. 2002.
- [6] T. J. Carpenter, R. C. Menendez, D. F. Shallcross, J. Gannett, J. Jackel, and A. V. Lehmen, "Maximizing the transparency advantage in optical networks," in *Proc. OFC'03*, 2003, MF88.
- [7] X. Yang and B. Ramamurthy, "Sparse regeneration in translucent wavelength-routed optical networks: Architecture, network design and wavelength routing," *Photon. Netw. Commun.*, vol. 10, no. 1, pp. 39–53, Jan. 2005.

- [8] G. Shen, W. V. Sorin, and R. S. Tucker, "ASE-noise limited cross-layer design for Island-based translucent optical networks," *IEEE J. Lightw. Technol.*, to be published.
- [9] G. Shen and W. D. Grover, "Segment-based approaches to survivable translucent network design under various ultra long haul system reach," *J. Opt. Netw.*, vol. 3, no. 1, pp. 1–24, Jan. 2004.
- [10] K. Zhu, H. Zhang, and B. Mukherjee, "Design of WDM mesh network with sparse grooming capability," in *Proc. Globecom'02*, 2002, pp. 2696–2700.
- [11] W. Yao, M. Li, and B. Ramamurthy, "Performance analysis of sparse traffic grooming in WDM mesh networks," in *Proc. ICC'05*, 2005, pp. 1766–1770.
- [12] B. Chen, G. N. Rouskas, and R. Dutta, "On hierarchical traffic grooming in WDM networks," *IEEE/ACM Trans. Netw.*, vol. 16, no. 5, pp. 1226–1238, Oct. 2008.
- [13] J. Strand, A. L. Chiu, and R. Tkach, "Issues for routing in the optical layer," *IEEE Commun. Mag.*, vol. 39, no. 2, pp. 81–87, Feb. 2001.
- [14] M. Wu and W. I. Way, "Fiber nonlinearity limitations in ultra-dense WDM systems," *IEEE J. Lightw. Technol.*, vol. 22, no. 6, pp. 1483–1498, Jun. 2004.
- [15] R. Ramaswami and K. Sivarajan, *Optical Networks: A Practical Perspective*, 2nd ed. San Francisco, CA: Morgan Kaufmann, 2002.
- [16] Data Sheet of 100 GHz-40ch Athermal AWG Module (Gaussian Type), PS701, FITEL.
- [17] Data Sheet of DiamondWave PXC, Calient Networks.



Gangxiang Shen (S'98–M'99) received the B.Eng. degree from Zhejiang University, Hangzhou, China, the M.Sc. degree from Nanyang Technological University, Singapore, and he received the Ph.D. degree from the Department of Electrical and Computer Engineering, University of Alberta, Edmonton, AB, Canada, in January 2006.

He is a Lead Engineer with Ciena, Linthicum, MD. Before he joined Ciena, he was an Australian ARC Postdoctoral Fellow with ARC Special Research Centre for Ultra-Broadband Information Networks,

Department of Electrical and Electronic Engineering, University of Melbourne, Melbourne, Australia. His research interests are in optical networks, network survivability, and hybrid wireless and optical networks. He has authored and coauthored more than 40 peer-reviewed technical papers.

Dr. Shen is a recipient of the Izaak Walton Killam Memorial Award from the University of Alberta, and the Canadian NSERC Industrial R&D Fellowship.



Rodney S. Tucker (S'72–M'75–SM'85–F'90) received the B.E. and Ph.D. degrees from the University of Melbourne, Melbourne, Australia, in 1969 and 1975, respectively.

He is a Laureate Professor at the University of Melbourne. He is director of the Australian Research Council Special Research Centre for Ultra-Broadband Information Networks in the University of Melbourne's Department of Electrical and Electronic Engineering. He has held positions at the University of Queensland, the University of California, Berkeley, Cornell University, Plessey Research, AT&T Bell Laboratories, Hewlett Packard Laboratories, and Agilent Technologies.

Prof. Tucker is a Fellow of the Australian Academy of Science, the Australian Academy of Technological Sciences and Engineering, and the Optical Society of America. In 1997 he was awarded the Australia Prize for his contributions to telecommunications. In 2007 he received the IEEE LEOS Aron Kressel Award for his contributions to high-speed semiconductor lasers.